

# An Adaptive Algebraic Dynamic Multilevel (A-ADM) and Multiscale Method with Enriched Basis Functions for the Simulation of Two-Phase Flows in Highly Heterogeneous Petroleum Reservoirs

José Cícero Araujo dos Santos<sup>1</sup>, João Paulo Rodrigues de Andrade<sup>2</sup>, Artur Castiel Reis de Souza<sup>1</sup>, Ricardo Jorge Morais de Lira Filho<sup>1</sup>, Darlan Karlo Elisiário de Carvalho<sup>2</sup>, Paulo Roberto Maciel Lyra<sup>2</sup>

<sup>1</sup>*Dept. of Civil Engineering, Federal University of Pernambuco*

*Av. Prof. Moraes Rego, 1235 - Cidade Universitária, Recife, 50670-901, Pernambuco, Brasil*

*josecicero.santos@ufpe.br, artur.castiel@ufpe.br, r.liraf@gmail.com*

<sup>2</sup>*Dept. of Mechanical Engineering, Federal University of Pernambuco*

*Av. Prof. Moraes Rego, 1235 - Cidade Universitária, Recife, 50670-901, Pernambuco, Brasil*

*jprandrade@gmail.com, darlan.ecarvalho@ufpe.br, paulo.lyra@ufpe.br*

**Abstract.** Classical Multiscale Finite Volume (MsFV) methods can produce highly oscillatory pressure solutions (i.e. non-monotonic) for high permeability contrasts. This can be a serious problem as it can produce spurious gas throughout the reservoir when the pressure erroneously falls below the bubble point pressure and it can substantially increase the computational cost to solve the problem due to the necessity of extensive use of iterative procedures in order to obtain a low-recirculation velocity field. In this paper, we propose an adaptive flow based agglomeration strategy for correcting the non-physical terms present in the coarse transmissibility matrix by means of a preprocessing local step. This is done by using a local recalculation of the basis functions in a patch defined by a judicious grouping of dual coarse volumes that eliminates the spurious oscillations. Classical multilevel and multiscale methods define a uniform level at each coarse control volume, i.e., the same mesh level is used at each coarse control volume. As a result, it generates, in multiphase transport problems, the necessity of the inclusion of volumes that do not contain the saturation front in the high-resolution level. In this context, we present a framework to deal with non-uniform levels at each coarse control volume, which allows the use of fine-scale control volumes only where it is strictly needed, in order to produce smaller coarse scale matrices than those from classical multilevel multiscale methods.

**Keywords:** Adaptive Algebraic Dynamic Multilevel (A-ADM), Algebraic Multiscale Solver (AMS), Multiscale Finite Volume (MsFV), Basis function enrichment, Adaptive non-uniform multilevel resolutions.

## 1 Introduction

The numerical simulation of fluid flow in petroleum reservoirs represents an important tool to obtain information that allows optimal ultimate oil recovery. The current industry standard for geocellular (static models) size up to  $10^9$  blocks, whilst simulation ready models (dynamic grids) size only up to  $10^7$  blocks. Thus, the simulation of flow on high resolution meshes is only possible through distributed computing systems [1] [2]. In general, techniques of homogenization, such as Upscaling, are applied to obtain approximated solutions using lower resolution meshes which implies in original data and accuracy loss. More recently, Multiscale Finite Volume (MsFV) methods were developed, as they provide more accurate solutions than those provided by Upscaling techniques, by transferring information between the fine and coarse scales using data transfer operators (restriction and prolongation), with reduced CPU cost when compared to fine-scale simulations. The prolongation operator is obtained through local solutions of elliptic problems with Reduced Boundary Conditions (RBCs). It's well known in literature that the RBCs, despite of allowing the fine-scale decoupling in local distributable problems, can lead to highly non-monotone pressure solutions, especially on highly heterogeneous reservoirs [3]. In this work we present the Adaptive Algebraic Multiscale Solver (A-AMS) which adapts the RBCs throughout agglomeration of

dual volumes in order to control the non-physical terms at the coarse-scale transmissibility matrix, by means of a preprocessing step. In addition, multilevel operators and level definition criteria are established and applied over a non-uniform mesh resolution. These criteria are based on the Adaptive Algebraic Multiscale Solver (A-AMS) prolongation operator and controls the non-physical terms at the Adaptive Algebraic Dynamic Multilevel (A-ADM) transmissibility matrix. The proposed methodologies are applied for the simulation of two-phase flow in petroleum reservoirs with highly heterogeneous permeability fields. Some remarkable results, as the reduction of pressure error norm, the infinity norm in three orders of magnitude and the Euclidian norm by a factor of 85, in comparison with the traditional AMS [1], was observed.

## 2 Mathematical model

In this article, we assume immiscible, isothermal and incompressible flow of oil and water with neglecting capillarity, gravity and adsorption through a non-deformable porous media and employ an implicit pressure explicit saturation (IMPES) strategy to solve the flux and transport equations. In this formulation, the pressure and saturation equations are solved separately in two different steps, coupled through the velocity field [4].

$$\begin{cases} -\nabla \cdot (\lambda^t \nabla p^{t+\Delta t}) = q \\ \phi \frac{\partial}{\partial t} S_\alpha^{t+\Delta t} = q_\alpha - \nabla \cdot (\lambda_\alpha^t \nabla p^{t+\Delta t}) \end{cases} \quad (1)$$

where  $\phi$  is the porosity of the media,  $p$  is the total pressure and  $S_\alpha$ ,  $\vec{v}_\alpha$  and  $q_\alpha$  denotes, respectively, the saturation, velocity and source/sink terms of the phase  $\alpha$ , with  $\alpha = o$  for oil and  $\alpha = w$  for water phase.  $\lambda = \lambda_o + \lambda_w$  is the total mobility, where  $\lambda_\alpha$  is the mobility of the phase  $\alpha$ . The problem described by the system of equations (1), requires an appropriate set of boundary conditions and initial conditions [4], which depends on the geological characteristics of the boundaries of the reservoir as well as the existence of injection and/or production wells.

## 3 Numerical approximation

Applying the finite volume method (FVM) in the fine-scale control volumes with fluxes calculated by the two-point flux approximation (TPFA) method [4], the flow problem of Eq. (1) can be written in matrix form as:

$$\mathbf{T}^f p^f = q^f, \quad (2)$$

where  $\mathbf{T}^f$  is the transmissibility matrix,  $p^f$  is the unknown pressure and  $q^f$  is a vector that represents boundary conditions and source/sink terms. The entries of  $\mathbf{T}^f$ ,  $\tau_{ij}^f$ , are associated to each internal face  $ij$  adjacent to the volumes  $i$  and  $j$  of the mesh, expressed as,  $\tau_{ij}^f, i \neq j = (\lambda_{ij} k_{ij} A_{ij}) / h_{ij}$ , where,  $\lambda_{ij}$  is the total mobility,  $h_{ij}$  is the displacement vector that links the adjacent volume centroids,  $A_{ij}$  is the  $ij$ 's area and  $k_{ij}$  is the harmonically averaged permeability on  $ij$ .  $\tau_{ij}^f, i=j = -\sum_{j=1}^{N_f} \tau_{ij}^f, i \neq j$  [2].

Moreover, by applying the Euler forward discretization for temporal term and first order upwind method (FOUM) [3] for the flux term we explicitly solve the transport problem, for the phase w:

$$S_w^{t+\Delta t} = S_w^t + \frac{\Delta t}{\phi} \cdot \left( \frac{\lambda_w^t}{\lambda^t} \mathbf{K} \nabla p^{t+\Delta t} \right) \quad (3)$$

where,  $\mathbf{K}$  is the permeability tensor. To guarantee stability of the transient problem, we need to limit the time step by the Courant-Friedrichs-Lewy (CFL) condition [6] which states that for linear stability,  $CFL = \Delta t (v_{ij,x} / h_{ij,x} + v_{ij,y} / h_{ij,y}) \leq 1$ , so the time step is set as:  $\Delta t = CFL (v_{ij,x} / h_{ij,x} + v_{ij,y} / h_{ij,y})^{-1}$ ,  $CFL \leq 1$ .  $\vec{v}_{ij} = -\lambda_{ij} \mathbf{K} \nabla p$  is the Darcian velocity vector.

## 4 Adaptive Algebraic Dynamic Multilevel (A-ADM)

### 4.1 The AMS multiscale method

The AMS (Algebraic Multiscale Solver) [7] performs scale transfers throughout restriction and prolongation operators. Two auxiliary meshes are used to define these operators: the primal and the dual meshes. The fine-scale control volumes within the dual coarse scale mesh, in 2D, are subdivided in three volume classes: Faces, Edges

and Vertices. Fig. 1 illustrates these different volume classes and the auxiliary meshes constructed on a fine-scale 2D mesh,  $\Omega$ , and highlights a primal coarse volume,  $\Omega^C$ , and a dual coarse volume,  $\Omega^D$ .

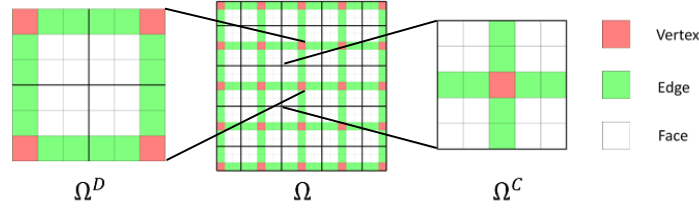


Figure 1: Illustration of AMS primal (bold lines) and dual coarse meshes superimposed to a 2D fine-scale mesh (tight gray lines),  $\Omega$ .  $\Omega^C$  is a primal coarse control volume, and  $\Omega^D$  a dual coarse volume.

The AMS approximates the fine-scale pressure solution,  $p^f$  of Eq. (5), by the multi-scale pressure solution,  $p^{ms}$ , which in turn is obtained from a linear combination of the coarse scale pressure solution,  $p^c$ ,

$$p^f \approx p^{ms} = \sum_{K=1}^{N_c} \Phi^K p_K^c = \mathbf{P} p^c. \quad (4)$$

This combination is expressed by the prolongation operator  $\mathbf{P}$ , a matrix with dimension  $n_f \times n_c$ . We obtain  $\Phi^K$ , the basis function associated to the  $K^{th}$  primal coarse scale volume, by solving in each dual coarse volume the decoupled local elliptic problem [8],

$$\begin{cases} -\nabla \cdot (\lambda \cdot \mathbf{K} \nabla \Phi^K) = 0 & \text{on } \Omega^D \\ -\nabla_{\parallel} \cdot (\lambda \cdot \mathbf{K} \nabla \Phi^K)_{\parallel} = 0 & \text{at } \partial \Omega^D, \\ \Phi^K = \bar{\delta}_{KL}, & \forall L \in [1, N_c] \end{cases} \quad (5)$$

Here, in the dual volume,  $\Omega^D$ , a local elliptic problem is solved, in the boundary of this dual volume,  $\partial \Omega^D$ , (Edge volumes) we impose the tangential flow. In the Vertex volumes we impose the Dirichlet boundary conditions [8]. The parameter  $\bar{\delta}_{KL}$  is the Kronecker delta,  $\bar{\delta}_{KL, K=L} = 1$ ,  $\bar{\delta}_{KL, K \neq L} = 0$ . It is worth to mention that the Dirichlet boundary conditions are applied over the Vertex volumes,  $V$ .

We can write the prolongation operator,  $\mathbf{P}$ , following the steps described by [7], as:

$$\mathbf{P} = \mathbf{G} \begin{bmatrix} \Phi_{FV} \\ \Phi_{EV} \\ \Phi_{VV} \end{bmatrix} = \mathbf{G} \begin{bmatrix} \mathbf{T}_{FF}^{-1} \mathbf{T}_{FE} \mathbf{T}'_{EE}^{-1} \mathbf{T}_{EV} \\ -\mathbf{T}'_{EE}^{-1} \mathbf{T}_{EV} \\ \mathbf{I}_{VV} \end{bmatrix}, \quad (6)$$

where:  $\mathbf{G}$  is the permutation matrix, responsible for the mapping of the Wirebasket ordering into the original volume ordering;  $\Phi_{AV}$  is the slice of the prolongation operator that linearly combines the Vertex pressures into the pressure on the volumes of the dual class A;  $\mathbf{T}_{AB}$  is the slice of the transmissibility matrix corresponding to the dual classes A and B respectively;  $\mathbf{I}_{VV}$  is the identity matrix with order  $n^c \times n^c$  and ,  $B = \text{Face (F), Edge (E), Vertex (V)}$ .

Substituting Eq. (6) on Eq. (4), and applying the restriction operator to both sides of the resulting equation, the coarse scale pressure problem can be written as:

$$\underbrace{\mathbf{RTP}}_{\mathbf{T}^c} p^c = \underbrace{\mathbf{R}q^f}_{q^c}. \quad (7)$$

In Eq. (7),  $\mathbf{R}$  is the restriction operator that integrates/summates, for each primal coarse volume, the fluxes of the correspondent fine-scale volumes [9].

The application of the RBC for the calculation of the basis functions, despite allowing the decoupling of the flow problem, can lead to negative transmissibilities on the coarse scale system, Eq. (7). High values of these non-physical terms make the AMS returns highly non-monotonic pressure solutions [1].

## 4.2 Dual volumes agglomeration, A-AMS

To overcome the generation of non-physical terms at the coarse-scale transmissibility matrix we propose the Adaptive AMS (A-AMS). In this method, we recalculate the basis functions on agglomerated dual volumes avoiding the application of RBC which otherwise leads to big non-physical terms at the coarse-scale transmissibility matrix generated by the AMS. The identification of these agglomerated dual coarse volumes is

based on the non-dimensional parameter,  $\eta$ , defined by [3].  $\eta_{IJ}^l = \tau_{IJ}^c / \tau_{II}^c$ . Here,  $\eta_{IJ}^l$ , is associated to the adjacent primal coarse volumes  $I$  and  $J$  in relation to line  $l$  and the unique,  $\eta$  parameter is taken as,  $\eta_{IJ} = \max(\eta_{IJ}^l, \eta_{JI}^l)$ . A threshold value,  $\varepsilon$ , is used to define the critical adjacencies, where  $\eta_{IJ} > \varepsilon$ . Once classified the critical adjacencies, we turn the crossing dual Edges into Faces through the agglomeration of dual volumes. Figure 2 shows the dual mesh from A-AMS superimposed to the permeability field for:  $\varepsilon = \infty$  (coincides with AMS), (a);  $\varepsilon = 1$ , (d). The agglomeration parameter, (b), and the agglomeration sets corresponding to  $\varepsilon = 1$ , (e). Four different basis functions for the original AMS (A-AMS with  $\varepsilon = \infty$ ), (c) and the same basis functions with  $\varepsilon = 1$ , (f).

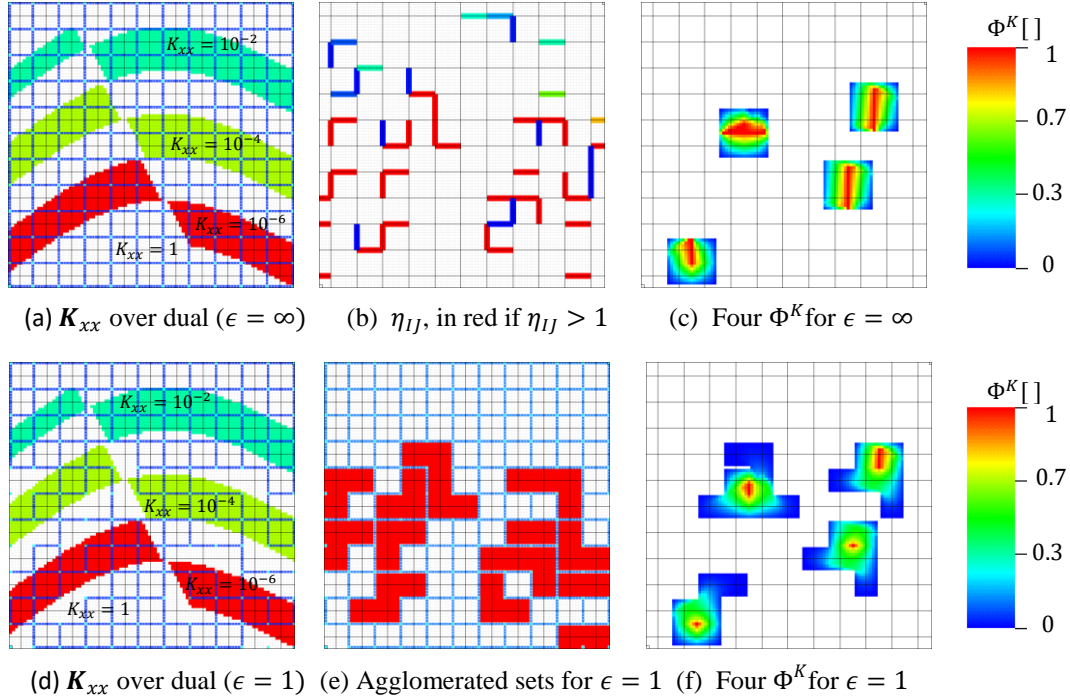


Figure 2: Illustration of the A-AMS dual adaptation: permeability field over the dual mesh (a) and (d); (b)  $\eta_{IJ}$ ; four different basis functions for: (c) AMS ( $\varepsilon = \infty$ ); (f) A-AMS ( $\varepsilon = 1$ ) and (e) agglomeration sets.

On the agglomerated dual volumes, even if we apply a TPFA scheme we have adjacencies between the Face and Vertex volumes so  $\mathbf{T}_{FV}$  is non-null and the prolongation operator have the following expression:

$$\mathbf{P} = \mathbf{G} \begin{bmatrix} \Phi_{FV} \\ \Phi_{EV} \\ \Phi_{VV} \end{bmatrix} = \mathbf{G} \begin{bmatrix} \mathbf{T}_{FF}^{-1}(\mathbf{T}_{FE}\mathbf{T}'_{EE}^{-1}\mathbf{T}_{EV} - \mathbf{T}_{FV}) \\ -\mathbf{T}'_{EE}^{-1}\mathbf{T}_{EV} \\ \mathbf{I}_{VV} \end{bmatrix}. \quad (8)$$

To increase computational efficiency, the basis functions are not updated during the transport problem solution. To maintain the accuracy along the simulation, we propose an Adaptive Algebraic Dynamic Multilevel (A-ADM) framework with a non-uniform adaptive mesh resolution.

### 4.3 Dynamic adaptation of the non-uniform multilevel resolution

In this work, we use the dynamic adaptation of the multilevel resolution to maintain the non-physical terms under control. We define a non-uniform multilevel resolution in order to reduce the non-physical terms at the coarse-scale transmissibility matrix,  $T^{A-ADM}$ . The level to which the fine-scale volume belongs is defined by three level-definition criterions:

The first compares the saturation variation between the adjacent volumes  $i$  and  $j$ ,  $\delta_{ij}$ , with a user defined threshold value,  $\delta_{ij}^{lim}$ . If  $\delta_{ij} > \delta_{ij}^{lim}$ , the volumes  $i$  and  $j$  are maintained on the fine-scale level.  $\delta_{ij} = \text{abs}(S_i - S_j)$

The second criterion compares the maximum ratio between the non-physical contributions to the off-diagonal terms of the coarse scale transmissibility matrix and the corresponding diagonal term,  $\alpha_i$ , with a user-defined threshold value,  $\alpha_i^{lim}$ . If  $\alpha_i > \alpha_i^{lim}$ , the volume  $i$  is maintained on the fine-scale level,  $\alpha_i = \max((\mathbf{T}^f \mathbf{P})_{i,K \neq I} / t_{II}^c)$ .

Finally, the third criterion avoids that the level of discontinuity leads to big non-physical terms at the multi-level transmissibility matrix. For fine-scale volumes  $i$  with small values of corresponding basis function  $\Phi_{I(i)}$  with

neighbors in the same condition, when some of them are kept on the fine-scale and the others are not, considerable non-physical terms may appear. Therefore, we group adjacent volumes for which  $\beta_i > \beta^{lim}$ , when some volumes in a group remain on the fine-scale, the entire group does the same.  $\beta_i = (\mathbf{1} - \Phi_{I(i)})/\Phi_{I(i)}$  and  $\beta^{lim}$  is a user defined threshold.

The multi-level resolution is used to solve implicitly the flow problem. The transport problem is solved explicitly on the fine-scale after an additional step for getting a conservative velocity field on the fine-scale, for further details about this step the reader is referred to [10].

## 5 Results

In this section, we present the results,  $x^{A-ADM}$ , obtained by applying the A-ADM framework to a set of test cases and compare to those obtained solution on the fine-scale mesh,  $x^{fs}$ . The error norm is defined as,  $\|e_x\| = \|x^{A-ADM} - x^{fs}\|/\|x^{fs}\|$ .

In the example we have used a fixed coarsening ratio  $CR = (5, 11)$  on the non-boundary coarse volumes. On the boundary coarse volumes the coarsening is adapted in order to create as uniform dual volumes as possible, in addition, we locate the dual vertex volumes on the external boundary of the domain similarly to [3] [10] [11].

To illustrate the influence of the previously defined dual agglomeration parameters and refinement criteria we have applied the A-ADM methodology to the CSP-SPE-10 (Comparative Solution Problem) [12] bottom layer, a reservoir with  $60 \times 220$  volumes and aspect ratio of  $A_r = 2$  ( $\Delta x = 2\Delta y$ ), with two wells. These wells are an injector with prescribed flow ( $10m^3/d$ ) at the bottom left corner and a producer with prescribed pressure ( $p = 50MPa$ ) at the top right corner. The permeability field and the wells positions are shown in Fig. 3. As initial condition we set a constant water saturation of  $S_w = 0.2$  equal to the irreducible, the residual oil saturation was set as 0.2, was used the Brooks and Corey model for relative permeability calculation. The viscosity was adopted as 0.3 cP for the water and 3cP for the oil, in addition null flux was set in all external boundaries.

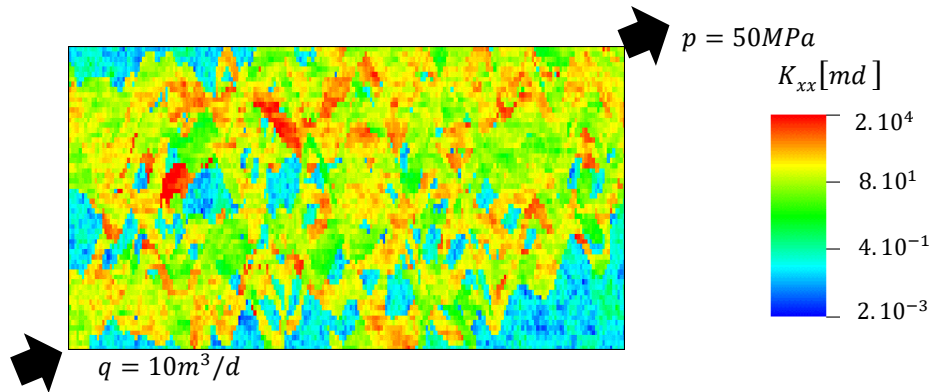


Figure 3. Permeability field of the CSP-SPE-10 bottom layer and wells localization, an injector with prescribed flow at the bottom left corner, and a producer with prescribed pressure at the top right corner.

Below, we present some observations made by observing the influence of the threshold value,  $\epsilon$ , for A-AMS on the accuracy of pressure solution and the amount of volumes in which the basis functions are recalculated:

- when  $\epsilon = \infty$  our method matches with the AMS because none dual volume is agglomerated;
- The Euclidian error norm of the pressure ( $\|e_p\|_2$ ) reduces from 85% to: 1% when  $\epsilon = 10$  or  $\epsilon = 1$ ;
- The maximum error norm for pressure ( $\|e_p\|_\infty$ ) reduces from 3000% when  $\epsilon = \infty$  to: 7% when  $\epsilon = 10$  and 3% when  $\epsilon = 1$ ;
- We recalculate 15% of the basis functions when  $\epsilon = 10$  and 27% when  $\epsilon = 1$ .

Qualitatively, the effect of the A-AMS can be observed for the pressure surface plots in Fig. 4. In this figure, we can observe the pressure spurious oscillations generated by the non-physical terms at the AMS ( $\epsilon = \infty$ ) solution, these artificial oscillations are significantly reduced when we apply the A-AMS with  $\epsilon = 10$  and disappear when we use  $\epsilon = 1$ .

For two-phase transport solution we have applied the A-ADM with two sets of refinement parameters, the first one included the criterion that considers the saturation field,  $\delta^{lim} = 0.1$ , and the second one does not,  $\delta^{lim} = \infty$ . Both cases used the A-AMS prolongation operator obtained with the agglomeration parameter  $\epsilon = 1$ ,



the maximum non-physical contribution to the coarse scale was limited by the threshold value  $\alpha^{lim} = 1$ , and the level discontinuity is limited by  $\beta^{lim} = 3$ . Figure (5) shows the porous volume injected versus the Euclidean pressure error norm, (a); percentage of active volumes (b) and water/oil ratio. Figure (6) shows the saturation front at the time-step corresponding to 0,3 PVI (Porous Volume Injected) for different flow solutions: obtained directly at the fine-scale, (a); obtained with A-ADM superimposed to the corresponding resolution for  $\delta = 0.1$ , (b); and for  $\delta = \infty$ , (c).

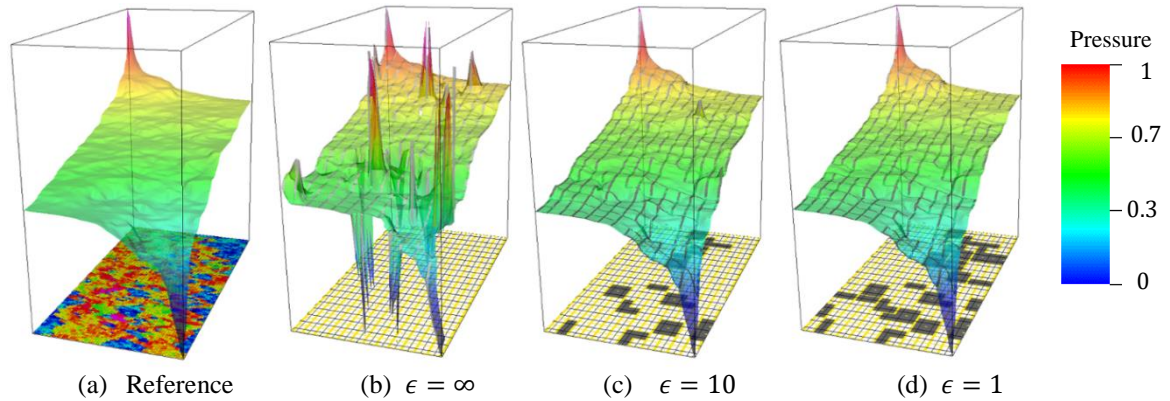


Figure 4. Pressure surface plots obtained with: the fine-scale over the permeability field, (a); the A-AMS over the dual mesh, for  $\epsilon = \infty$ , (b);  $\epsilon = 10$ , (c);  $\epsilon = 1$ , (d).

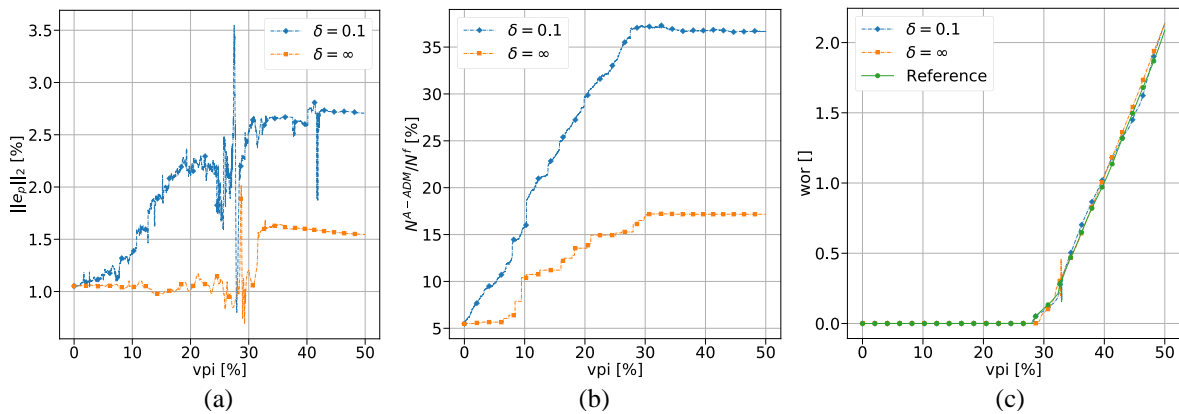


Figure 5. Porous volume injected (PVI) versus: Euclidean error norm for pressure, (a); percentage of active volumes, (b); and water/oil ratio, (c).

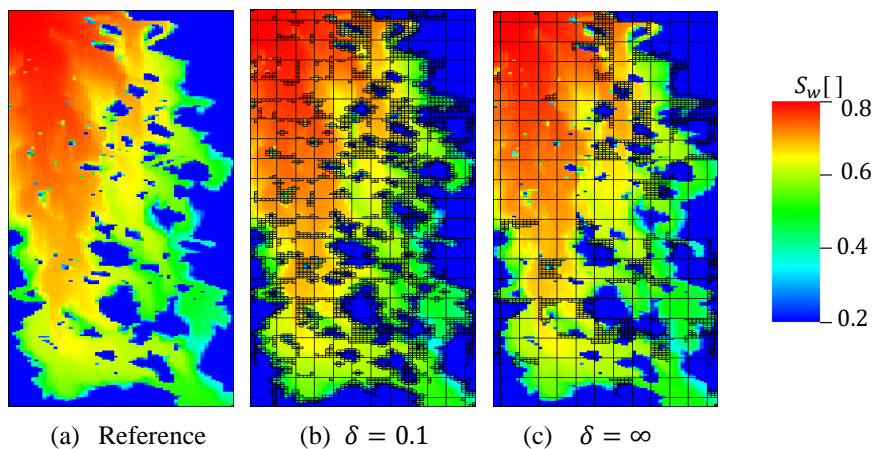


Figure 6. Saturation front at the time-step corresponding to 30% of porous volume injected for: a) solution at fine-scale, and A-ADM mesh, superimposed to corresponding saturation front for: b) A-ADM including saturation based parameter; c) A-ADM, without saturation based parameter.

## 6 Conclusions

In this paper, we have proposed an Adaptive Algebraic Dynamic Multilevel (A-ADM) method. By means of new mesh level definition criteria, the method uses a non-uniform mesh resolution to control the non-physical terms that may induce non-monotone solutions at the A-ADM transmissibility matrix along the simulation. We also have proposed A-ADM operators that are constructed with the Adaptive Algebraic Multiscale Solver (A-AMS) operators. The results obtained for single phase and two phase simulations shown that the A-ADM framework is capable of producing accurate results for a challenging problem (bottom layer of SPE-10) using only a fraction of the volumes of the original fine-scale problem.

**Acknowledgements.** We would like to thank FACEPE (Fundação de Amparo à Ciência e Tecnologia do Estado de Pernambuco) and CNPq (Conselho Nacional de Desenvolvimento Científico e Tecnológico) for the financial support for this research.

**Authorship statement.** The authors hereby confirm that they are the sole liable persons responsible for the authorship of this work, and that all material that has been herein included as part of the present paper is either the property (and authorship) of the authors, or has the permission of the owners to be included here.

## References

- [1] Y. Wang, H. Hajibeygi and H. A. Tchelepi, "Monotone multiscale finite volume method," *Comput Geosci*, pp. DOI 10.1007/s10596-015-9506-7, 2015.
- [2] A. J. Rosa, R. S. Carvalho and J. A. D. Xavier, Engenharia de reservatórios de petróleo, Rio de Janeiro: Interciência, 2006.
- [3] L. M. C. Barbosa, A. R. E. Antunes, P. R. M. Lyra and D. K. E. Carvalho, "An iterative modified multiscale control volume method for the simulation of highly heterogeneous porous media flow," *Journal of the Brazilian Society of Mechanical Sciences and Engineering*, vol. 71, pp. 1-17, 2018.
- [4] S. Bosma, H. Hajibeygi, M. Tene and H. A. Tchelepi, "Multiscale finite volume method for discrete fracture (MS-DFM)," *Journal of Computational Physics* 351, pp. 145-164, 2017.
- [5] H. T. H. Zhou, "Two-Stage Algebraic Multiscale," *SPE journal*, pp. 523-539, 2012.
- [6] A. C. R. d. Souza, L. M. C. Barbosa, F. R. L. Contreras, P. R. M. Lyra and D. K. E. d. Carvalho, "A Multiscale Control Volume framework using the Multiscale Restriction," *Journal of Petroleum Science and Engineering*, no. 188, 2020.
- [7] M. Christie and M. Blunt, "Tenth SPE Comparative Solution Project: A Comparison of Upscaling Techniques," *SPE Reservoir Evaluation & Engineering* 4, pp. 308-317, 2001.
- [8] L. M. C. Barbosa, Formulações multiescala localmente conservativas para a simulação de reservatórios de petróleo muito heterogêneos e anisotrópicos /Tese de doutorado, 163p, Recife, 2017.
- [9] R. Courant, K. Friedrichs and H. Lewy, "On the partial difference equations of mathematical physics," *IBM Journal of Research and Development*, pp. 215-234, 1967 [1928].
- [10] M. M. Dehkordi and M. Manzari, "Effects of using altered coarse grids on the implementation and computational cost of the multiscale finite volume method," *Adv Water Resour*, pp. 221-237, 2013.
- [11] R. Künze, I. Lunati and S. H. Lee, "A Multilevel Multiscale Finite-Volume Method," *Journal of Computational Physics*, pp. 502-520, 2013.
- [12] E. Parramore, M. G. Edwards, M. Pal and S. Lamine, "Multiscale Finite-Volume CVD-MPFA Formulations on Structured and Unstructured Grids," *Multiscale Modeling & Simulation* 14.2, pp. 559-594, 2016.
- [13] H. T. H. A. Zhou, "Operator-based Multi-scale Method for Compressible Flow," *Society of Petroleum Engineering Journal*, v. 13, pp. 267-273, 2008.